EXTRACTING INFORMATION FROM DIGITAL IMAGES OF CORE

Craig Phillips, Rocco DiFoggio, Kathryn Burleigh
Core Laboratories

ABSTRACT

Quantitative image analysis is becoming routine as digital images gain popularity. The trend seems to be accelerating each year, as the cost to create, store, and process digital images declines.

Digital images of core were captured in white, ultraviolet, and infrared light using a video camera or scanner. The ultraviolet and infrared images can be used to detect hydrocarbons, discriminate mineralogy, and to observe features of a rock through black crude oil covering its surface.

Digital images can be easily manipulated for presentation alongside conventional wireline logs and borehole images. Such presentations enhance the usefulness of both the wireline and core data. They can help the user orient the core, compensate for missing or lost sections, and rapidly calibrate logs.

Our image processing system can perform color discrimination of features in core images. It can be used to quantify the amounts of sand and shale. With our system, the user simply clicks one at a time on a handful of pixels in the image whose colors represent the range of colors exhibited by the feature of interest (e.g. tan-fluorescing oil sands). This trains the computer to recognize these selected colors and all similar colors.

This training process is implicit rather than explicit. Unlike other systems, the user doesn't have to worry about setting acceptance windows for red, green, and blue intensities. The user simply picks out the representative colors visually and lets the computer handle the mathematical details.

In this way, one can quantify various features such as percent fluorescing oil sands, number of sand or shale laminae, thicknesses of these laminae, and bedding angles to improve reservoir description and correlation to logs. Computer processing of images also relieves geologists of the tedious and often inaccurate task of trying to manually quantify these features.

INTRODUCTION

Digital images have many advantages over conventional photographs. They can be easily processed by computer and archived in central databases where they can be accessed simultaneously by multiple users. In principle, they have an infinite non-degrading lifetime.

That is, their lifetime can exceed that of the medium on which they are stored because they can be copied without degradation to a new medium long before the old medium has physically degraded.

Digital imagery holds great potential for core analysis and reservoir description. Images of slabbed core or thin sections can be taken under white, ultraviolet, or infrared light to highlight various features of interest, such as oil-staining[1], lithology-related color changes[2,3,4], and mineralogy. These images can be displayed alongside the logs at any scale or aspect ratio for best visual comparison and can be processed to yield various parameters (e.g. percentage of sand) as a continuous function of depth.

With our image processing system (ImageLog), we have quantified features such as percentage fluorescing oil sands, number of sand or shale laminae, thicknesses of these laminae, and bedding angles. These capabilities are particularly useful in thinly-laminated reservoirs, where they substantially improve reservoir description.

ALGORITHMS FOR COLOR DISCRIMINATION

There are many algorithms for processing digital images. Most are intended for use with monochrome (gray scale) images and relate to contrast enhancement, noise reduction, morphological description, or object counting. These monochrome processing algorithms are often poorly equipped to extract the wealth of information contained in color images[5].

We have emphasized color discrimination image processing. The user visually selects a training set of various shades of color of some feature in the image (e.g., tan-fluorescing oil sands, see selected pixels circled in Figure 1a). The computer then recognizes these colors and all similar shades of color.

In our current configuration, each shade of color can have a red, green, and blue intensity value between 0 and 31 so that 32,768 color combinations are possible. In three-dimensional red-green-blue color space, the training set of colors that we select appears as a cloud of points (Figure 1b).

Most color discrimination algorithms simply surround the training set of colors in color space with a rectangular box[6] whose edges are parallel to the red, green, and blue axes. Colors inside the box are considered similar to the training set, and those outside are not.

However, the rectangular box approach ignores the covariance of the colors. That is, it ignores that the red, green, and blue components of the training-set colors do not vary independently of one another. For example, the various shades of tan-colored oil fluorescence under ultraviolet light typically have red and green components that are approximately equal and much greater than the blue component.

Stated another way the cloud of training set colors tends to be shaped like a cigar with axes that are not parallel to the red, green, and blue axes. This cloud of points typically lies diagonally across any rectangular box intended to surround it. Trying to model such a cloud of points with a rectangular box results in including many inappropriate colors, particularly those in the opposite corners of the box.

We chose to model the cloud of training set colors with an ellipsoid (Figure 1b) because it allows better color discrimination. The lengths of the ellipsoid axes and their directions are determined by principal component analysis.

We begin by computing the mean-centered covariance matrix of the training set of colors. Then, we compute the eigenvectors and eigenvalues of this matrix[7]. That is, we find a new rotated coordinate system that most appropriately describes the covariance between the red, green, and blue components.

The eigenvectors point along the directions of the axes of the new rotated coordinate system. They also point along the directions of the axes of the ellipsoid that best fits the cloud of points. The lengths of the ellipsoid axes are determined from the eigenvalues.

Next, the image is scanned pixel by pixel. Colors similar to the training set lie within this ellipsoid. Other colors do not. Figure 1c is a processed "binary" image in which selected pixels are shown in green and non-selected in blue. In this way, we can add up the percentage of the image that is similar in color to the training set and thus part of the selected feature.

We can also calculate the percentage of the selected feature that lies along lines parallel to the apparent dip and thus generate a continuous plot of percentage of the selected feature versus depth (Figure 2). This plot often correlates well with actual downhole logs. For example, when applied to oil-fluorescence under ultraviolet light this plot can be thought of as a "paylog" and correlates well with the downhole resistivity log.

TECHNOLOGY

The technology of digital imaging is advancing rapidly. Just a few years ago, a 256 color palette was considered average and 32,768 different colors (three 5-bit colors) was considered exceptional. Today, however, 16.7 million colors (three 8-bit colors) is emerging as the norm and we anticipate that, in a few more years, 1 billion colors (three 10-bit colors) will be available at a lower cost than today's systems.

Improved color resolution is just one example of how the technology in this area has leaped forward. There are several other concurrent

technological developments (including economics) that are responsible for the proliferation of imaging systems. These include larger capacity disk drives, color scanners, color printers, faster computers, and dedicated graphics chips.

The importance of more disk storage and faster computation becomes apparent when one considers the size of image files. A 5-bit per color red-green-blue (RGB) image at a spatial resolution of 512 x 512 pixels occupies a little over a half of a megabyte. If we raised the spatial resolution to 300 dots per inch, a single 8-1/2 by 11-inch image would occupy 16.7 megabytes.

There also has been a tremendous growth in software to generate, manipulate, and process images for various applications including Landsat, NMR, CT, and microbiology. Thus, we can incorporate relevant algorithms from other applications into our existing software as the need arises. Graphical user-interface software is now available for most computer platforms. This makes image processing more accessible to the novice or casual user.

One issue that remains to be resolved is standardization of image file formats in the petroleum industry. We currently support major file structures such as TIF, TGA, and GIF. We would support a petroleum industry standard if one were adopted. Such standardization would simplify creation of large image databases and allow easier sharing of images between oil companies that are partners on major projects.

APPLICATIONS

The applications of digital core image analysis are varied and have tremendous potential for log calibration and reservoir description. To improve integration of the data, the results of the image processing are tabulated and provided to the user in electronic format for use as input to other, more conventional, log analysis programs (Table 1).

Figure 3 shows a digital core image alongside the core photograph from which it was obtained. An advantage of the digital core image is that it can be readily presented at any scale to match the logs. With some effort, conventional photographs also can be produced at any scale, but the aspect ratio is fixed. Thus, when core photographs are reduced to the scale of logs, extremely narrow, unusable core images result.

Digital images, however, are not fixed to any aspect ratio. This allows the flexibility to view the image at any aspect ratio or scale. The processed data and digital core images become useful tools for reservoir description and log calibration.

Borehole Image Calibration

A wireline log-derived borehole image typically relies on acoustic or resistivity contrast. However, there are a number of factors such as stratigraphy, hole conditions and mud characteristics, that can affect the overall image quality.[8,9] There also may be other features present in the image that require interpretation. Both the digital core image and data measured from the core (e.g., fracture aperture, permeability and sand flag) can aid in the interpretation and validation of borehole images.

Figure 4 shows a statically-scaled Formation Micro-Scanner (FMS) image adjacent to the image of a core in a laminated sand/shale sequence. The FMS image is not optimally scaled; therefore, only the major sands have been imaged. After comparing the digital core image and the FMS, one operator decided to go back and rescale the borehole image to make it more representative of the core.

Figure 5 shows an acoustic Circumferential Borehole Imaging Log (CBIL, both amplitude and travel time) adjacent to the core image in a dense, fractured, carbonate reservoir. Here, the objective of the digital image comparison is to determine the type and extent of the fractures that the borehole image is capable of detecting.

In this example, the obvious sinusoids on the CBIL amplitude are immediately adjacent to the fractures described as open on the core (X465.5 and X470.0). The healed fractures are not detected (X467.0 and X471.0), and the fracture described as partially mineralized appears as a discontinuous sinusoid (X467.5) on the CBIL image.

This comparison allows us to determine that the continuity of the sinusoids is related directly to the degree to which the fractures are open. In addition, partially mineralized fractures observed in the core provide calibration for the fracture apertures of the borehole image.

The borehole image is easier to interpret after it has been calibrated to the core. This also improves the interpretation of the subsequent wells imaged in the same area and formation.

The Core Data and Conventional Logs

There is a tremendous benefit in being able to present the processed data or image from a core juxtaposed to the conventional well logs. A "low resistivity" sand may be no more than a thinly laminated sand/shale sequence. The dip oriented net/gross curve ("paylog") that is generated from the processed core images as well as the image itself can allow the log analyst or petrophysicist to understand the physical situation and compensate for it in the formation evaluation.

In conjunction with white light photography, the UV core images also can aid in reservoir description and well completion. Engineers can select zones for perforation based on evaluation of a fluorescence curve developed from processing fluorescing sands in a UV core image. The sand curve developed from the white light core image in non-fluorescing sands (i.e., gas bearing sands) can serve the same purpose.

Depth Alignment and Orientation of Core

Concatenated digital images can be very useful in depth shifting the core to the log and making adjustments for missing sections of core. Bedding, fractures, vugs, stylolites, and other structural features as well as coring-induced artifacts appearing on the digital core image and detected on the higher resolution logs can be used in the depth alignment process. Digital image depth shifting is a new technique that can be used to compliment the traditional core-to-log gamma ray, porosity, and resistivity techniques.

In addition, it is possible to orient the core to structural features indicated by the logs. This is a standard procedure; however, displaying the digital image of the core at the same scale as the log compliments, and in many instances, substantiates the final core orientation. This is possible mainly with oriented dipmeter and borehole imaging logs.

Referring again to Figure 5, it was possible to orient each open fracture seen on the core to the same azimuth, as indicated by the sinusoid on the borehole image. Figure 6a shows the pole plot of the open fractures from the amplitude image. Figure 6b shows the pole plot of the open core fractures as initially measured against an arbitrary orientation line. Comparing the digital image of the core to the borehole image provides a credibility factor in the orientation of the core. It is obvious that the open fractures seen on the core image are adjacent and related directly to the sinusoids; therefore, the open fractures have to have the same orientation. A scribe line correction is applied to the core segment to establish the correct orientation for each open fracture (Figure 6c). Finally, the same scribe line corrections are used between the core's spin surfaces to orient all the fractures to true magnetic north (Figure 6d).

Enhanced Digital Images

There are numerous instances when the actual core or core image is rather featureless. However, digital images can be enhanced to highlight features that would otherwise be difficult to see. Figure 7 shows a color photograph of a core (right) with a digital image from the same interval (left) enhanced to accentuate the difference between the sands and the shales. Here, the digital image is essentially a high-contrast binary image; however, on the original color photograph, the color differences were nearly indistinguishable.

Thin Bed Analysis

Quantitative analysis of thinly laminated sequences is one of the most challenging tasks in formation evaluation. Logging tools can be severely hampered by limited vertical resolution and/or depth of investigation. The processed data from ImageLog provides the information necessary to determine bed boundaries, thickness and frequency of laminae sequences. These data can be used with the conventional or high resolution logging suite to improve thin-bed evaluation.

Visual comparison of a core image to a borehole image is a purely qualitative process which provides no assessment of sand or shale volumes. One needs to quantitatively process the data of the digital image to aid this aspect of the evaluation.

Figure 8 shows the spherically focused shallow resistivity log (SFL) cross plotted against the average of all 16 buttons from Pad 1 of the FMS tool. The percent selected pixels along the apparent dip or "paylog" is on the Z axis and designated by the different colors of the sample markers (+) as seen on the cross plot. In essence, the black +'s (0 to 20% selected pixels) represent the shales and the red +'s (80 to 100% selected pixels) represent the sands. There appears to be a cluster of shale points below 4.0 ohm-meters on PAD 1 and 3.5 ohm-meters on the SFL. However, this cross plot includes all of the data. Some of the beds are too thin to be fully resolved by the shallow resistivity tool; therefore, there appears to be a lot of "noise".

To eliminate the noise, the same data were cross plotted, using the ImageLog "thickness" curve as a cutoff curve. Beds less than 1.0 foot were eliminated from the cross plot (see Figure 9). The shales cluster below 4 ohm-meters on PAD 1; therefore, a 4.0 ohm-meter cutoff was used to differentiate between sand and shale. Figure 10 shows how the predicted sand/shale ratios compare with those derived from the processed core images. To test the model, the same 4 ohm-meter threshold was used on another cored well in the field. The predictions were made, and then the core from the second well was digitally processed. The predicted results compared favorably to the processed data from the core (Figure 11).

SUMMARY/CONCLUSIONS

There are many benefits to capturing and processing digital images of core. Some of these are summarized below.

- It is now possible to do routine macroscopic analysis on images obtained from cores or core photographs.

- The process facilitates log-core integration and reservoir description.

- Core image analysis is readily applicable and beneficial to thin-bed analysis.

- Future applications include analysis of core images for quantitative lithologic and mineral volumes (e.g., anhydrite nodules, microporous chert or other features prominent on the core surface).

- The images can be stored on digital media for archival and multi-user purposes.

- Thin-bed analysis can be improved using the paylog, sand flag, and thickness data. The sand flag can also be used in cluster analysis.

- The paylog can be used to match various low-resolution logs to high resolution logs[10].

ACKNOWLEDGEMENTS

We would like to thank Pinky Vinson of BP Exploration and Bill Henry of Shell Offshore, Inc. for their suggestions, input and guidance during the development of this technology. Their help was invaluable. The Atlas Wireline's WDS Support group provided excellent assistance in tailoring their software to facilitate the integration of the digital core images with the other log and core data. We would also like to thank Dan Georgi for his assistance in the preparation of this paper and Core Laboratories for allowing us the time to dedicate to this project.

REFERENCES

1) Helander, Donald P. (1983), Fundamentals of Formation Evaluation, OGCI Publications, Tulsa.

2) Siegal, B. S. and Gillespie, A. R. (1980), Remote Sensing in Geology, Wiley Publishing, New York.

3) _____ (1989), Seventh Thematic Conference on Remote Sensing for Exploration Geology, Calgary, Alberta, Canada, Oct. 2-6.

4) _____ (1965), Ultraviolet and Fluorescence Photography, Vol 2, Focal Encyclopedia of Photography, Focal Press, New York.

5) Russ, John. C. and Russ, J. Christian (1990), Computer Imaging of Microscope Color Images, Scientific Computing and Automation, Vol 7, No 1, October.

6) Plice, R. K. (1988), Electronic Imaging Exposition and Conference, Summary of Papers Presented, Vol 2, p 689-694, Boston, October 3-6.

7) Collins, R. E. (1968), Mathematical Methods for Physicists and Engineers, Reinhold Publishing, New York.

8) Hackbarth, C. J. and Tepper, B. J., 1988, Examination of BHTV, FMS, and SHDT Images in Very Thinly Bedded Sand and Shales: Paper presented at the SPE Sixty-Third Annual Technical Conference and Exhibition, October 2-5, Houston, TX.

9) Ekstrom, M. P. et al., 1987, Formation Imaging with Microelectrical Scanning Arrays: The Log Analyst, May-June, pp. 294-306.

10) Nelson, R. J. and Mitchell, W. K., 1990, Improved Vertical Resolution of Well Logs by Resolution Matching: Paper presented at the SPWLA 31st Annual Logging Symposium, June 24-27, Lafayette, LA.

Table 1

OUTPUTS AVAILABLE FROM IMAGELOG

OUTPUT	DESCRIPTION	FORMAT
- Scanned Image File	- Original digital image	Image File
- Gray Scale Image (Derived from color image file)	- Brightness but no color	Image File
- "Binarized" Image File	- Selected pixels in green Non-selected in blue	Image File
- Processed Data		ASCII File
As Function of Depth	- Every 1/120 of a foot	
Dip Oriented Net/Gross	- Percentage selected pixels along the apparent dip	
Sand Flag	- 0 or 1	
Thickness	- Depth interval over which sand flag does not change	
Global Net/Gross	- Percentage selected pixels over entire processed area	

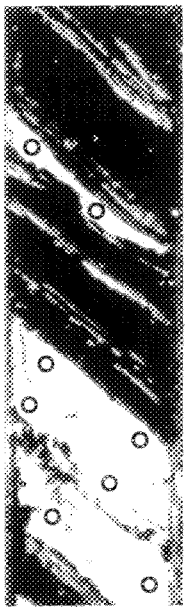

Figure 1a - Selected pixels used in the training set.

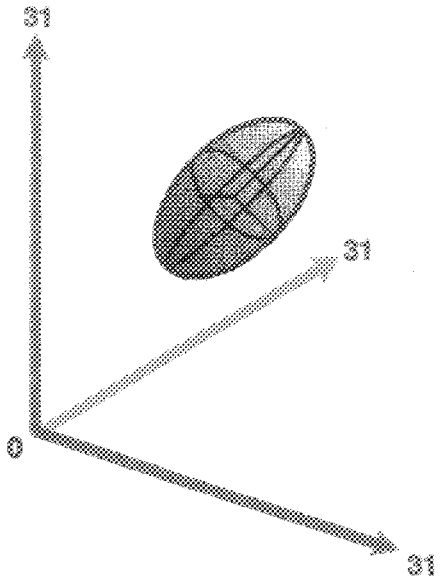

Figure 1b - The Elliptical Cloud calculated from the training set.

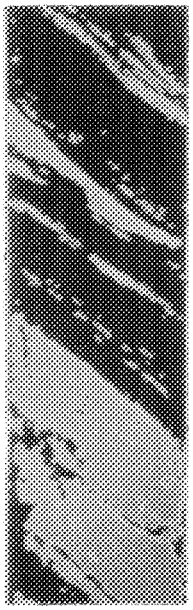

Figure 1c - Processed image with green representing colors within ellipsoid.

Figure 2 -

Top Depth	Bottom Depth	Selected Percent	Excluded Percent
1000.0	1001.0	67.5	32.5

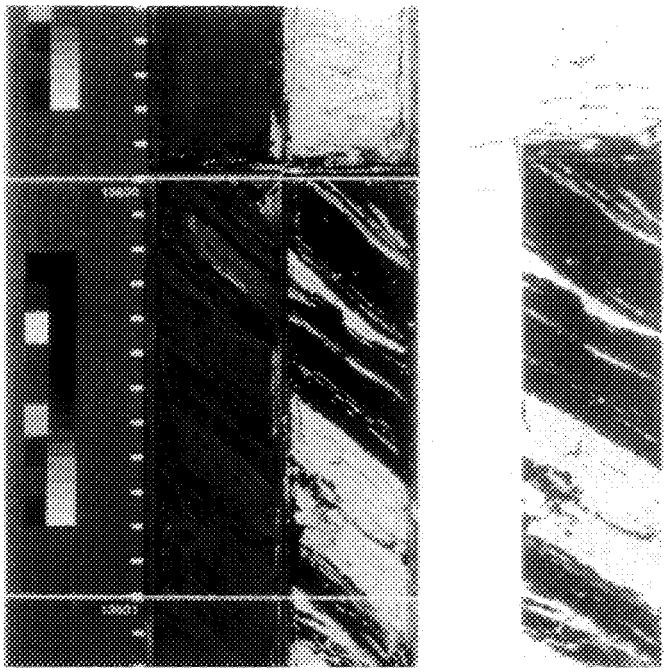

Figure 3 - Core Photographs with representative digital image.

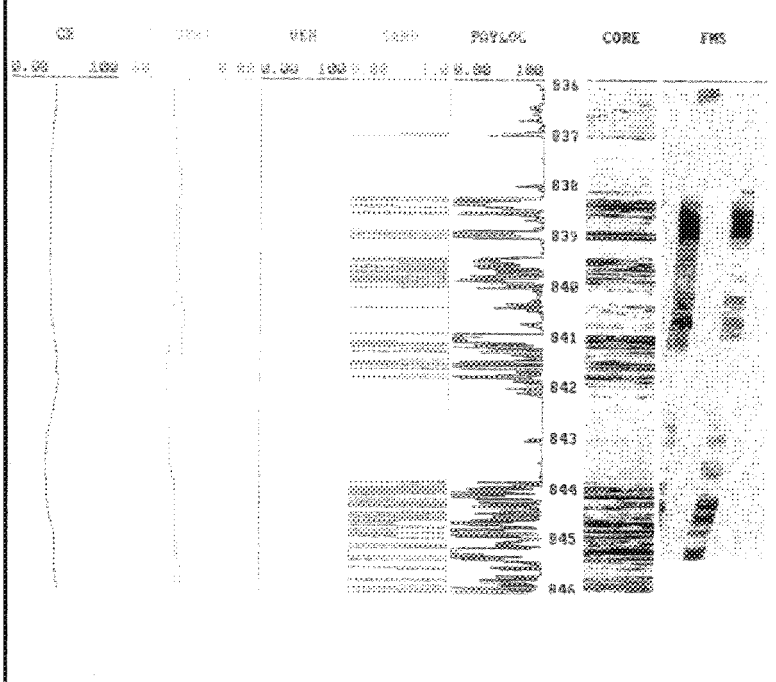

Figure 4 - Digital core image with FMS borehole image.

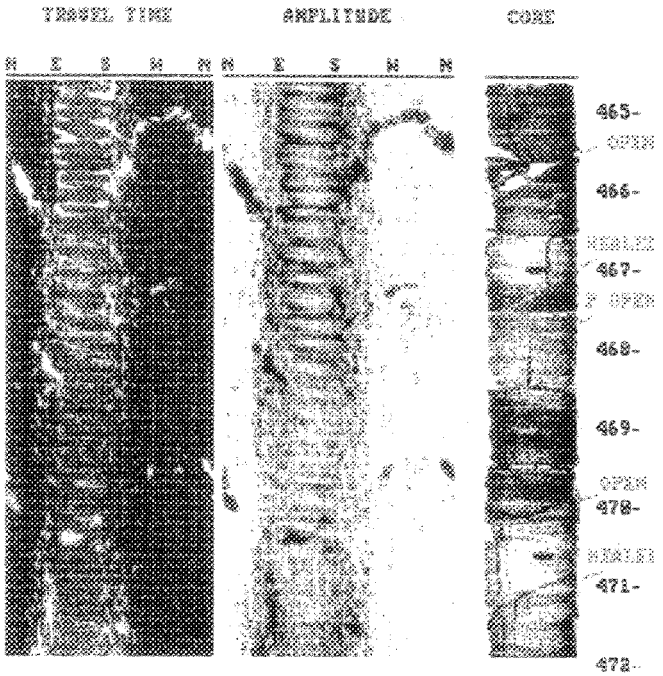

Figure 5 - Digital core image with CBIL borehole image.

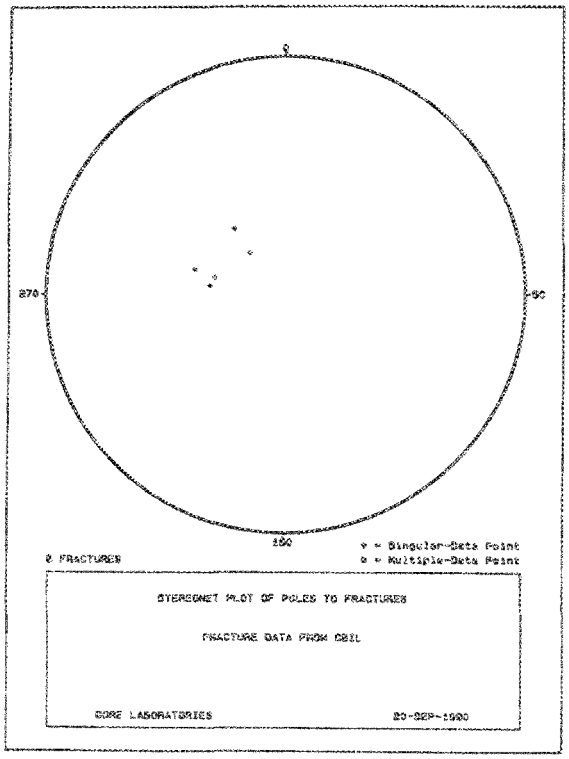

Figure 6a

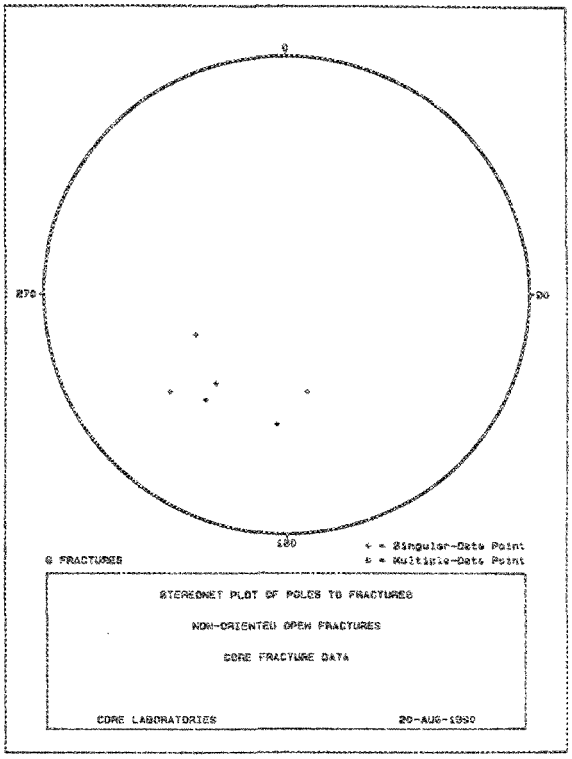

Figure 6b

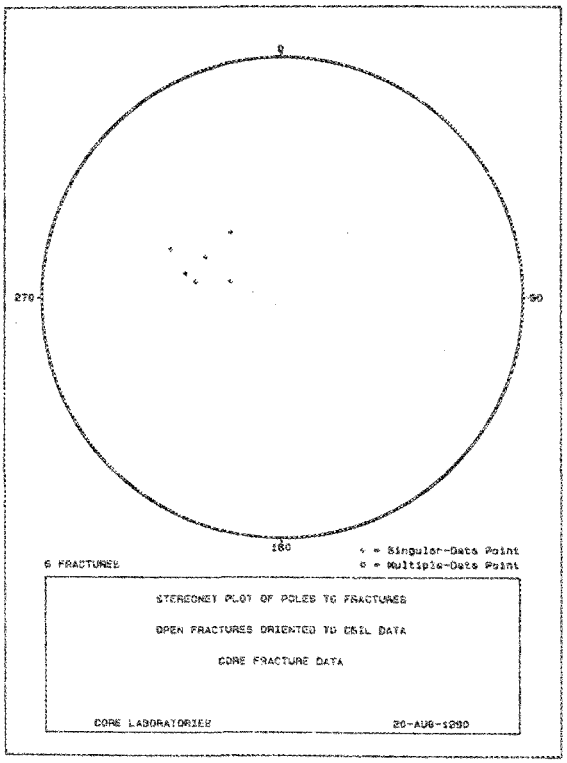

Figure 6c

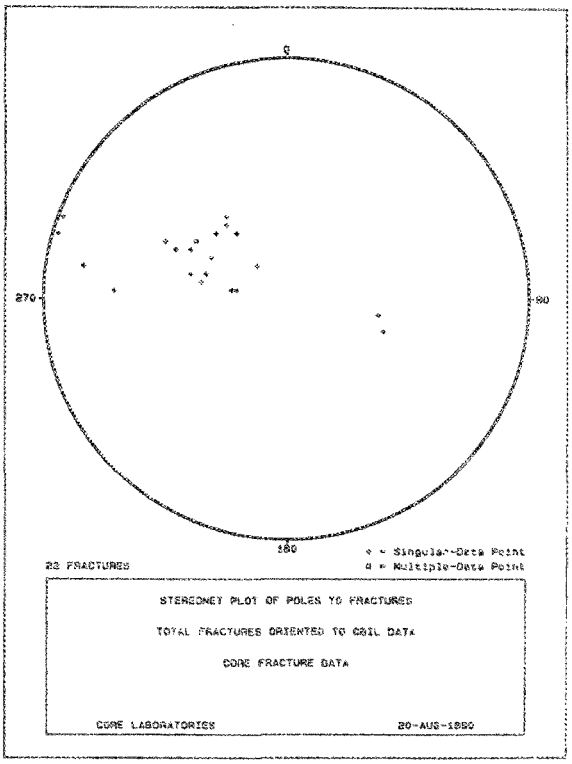

Figure 6d

Figure 6 - Pole plots of fractures from CBIL (6a), un-oriented core (6b), open core fractures oriented to CBIL (6c), and entire core oriented to the borehole image (6d).

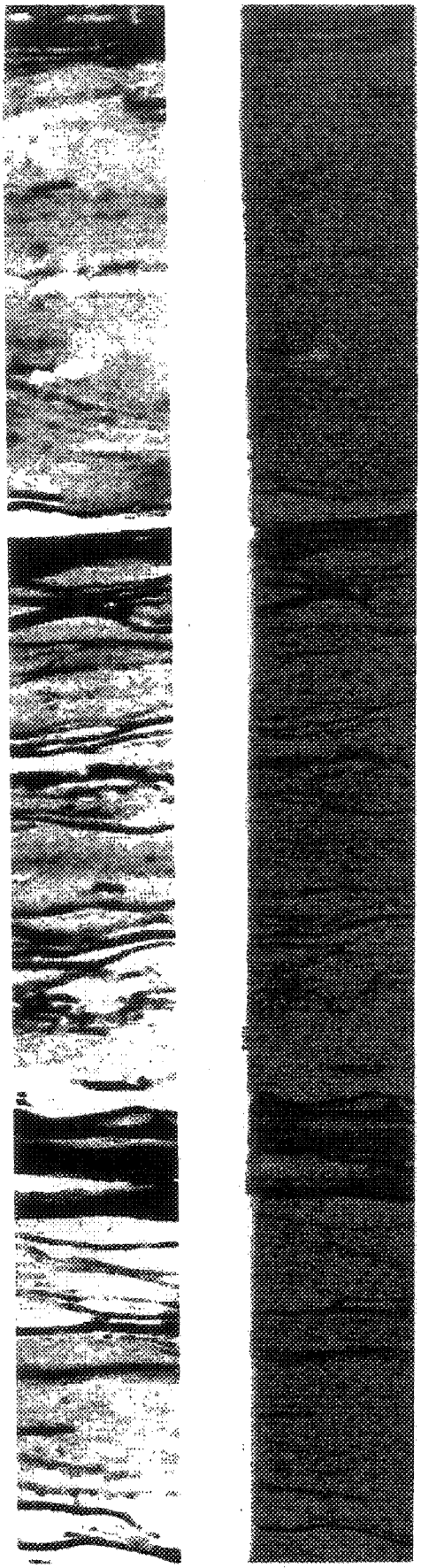

Figure 7 - Core photograph (right) with digital image (left) scaled to enhance the laminated nature of the formation.

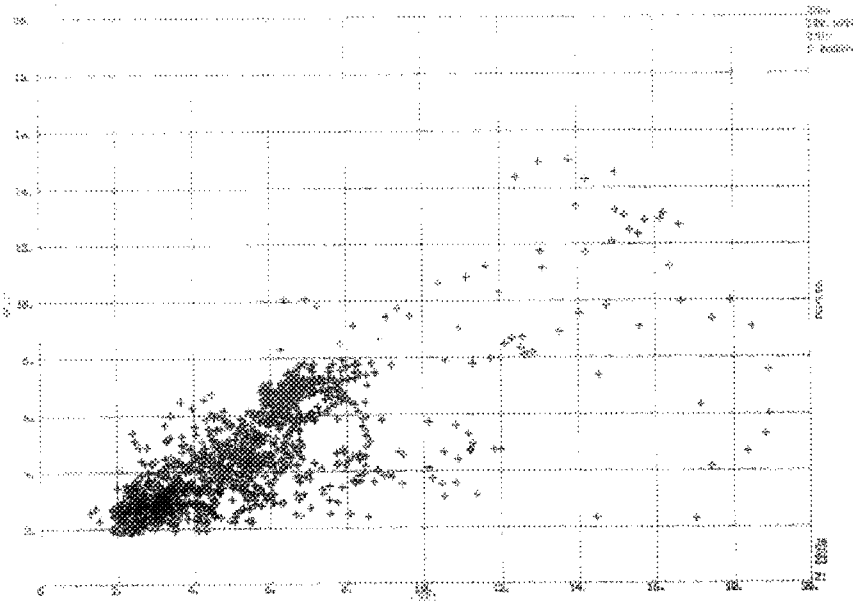

Figure 8 - SFL vs PAD1 of the FMS cross plot with paylog on the Z axis.

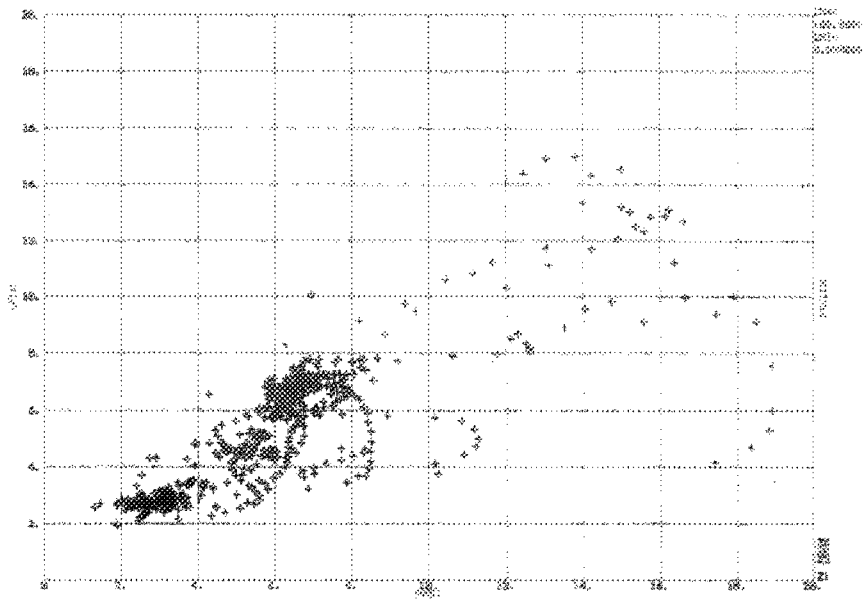

Figure 9 - SFL vs PAD1 of the FMS cross plot with paylog on the Z axis, however, a 1 foot thickness cut off was employed.

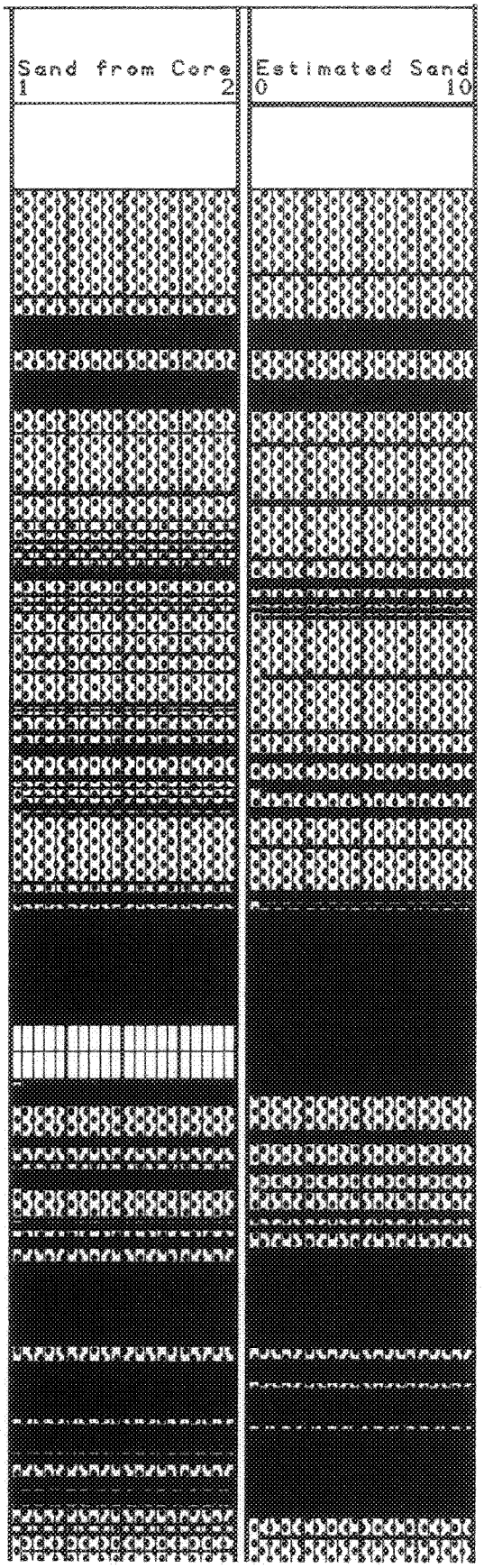

Figure 10 - The sand/shale from the core in comparison to a sand/shale prediction from the 4 Ohmm cut off on Well # 1.

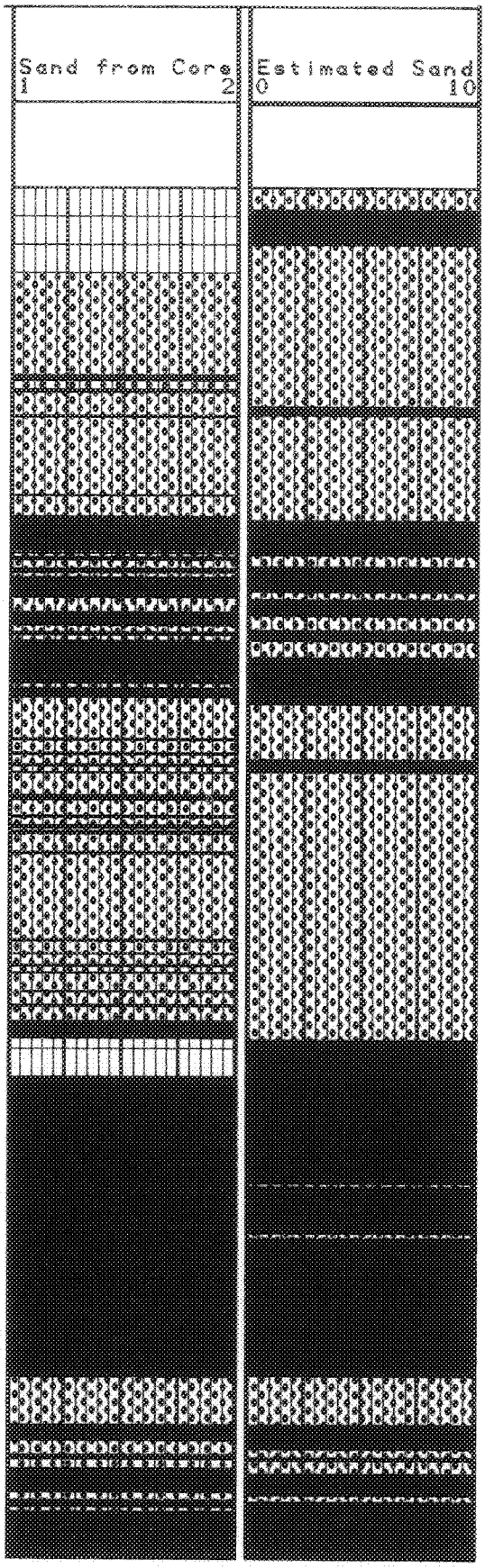

Figure 11 - The sand/shale from the core on Well # 2 in comparison to the sand/shale predicted with the same 4 Ohmm cut off.